blood®
Regular Article

LYMPHOID NEOPLASIA

Unexpected suppression of tumorigenesis by c-MYC via TFAP4-dependent restriction of stemness in B lymphocytes

Elena Tonc,[1] Yoshiko Takeuchi,[1] Chun Chou,[1] Yu Xia,[1] Melanie Holmgren,[1] Chika Fujii,[1] Saravanan Raju,[1] Gue Su Chang,[2] Masahiro Iwamoto,[3] and Takeshi Egawa[1]

[1]Department of Pathology and Immunology and [2]McDonnell Genome Institute, Washington University School of Medicine, St Louis, MO; and [3]Department of Orthopaedics, University of Maryland, Baltimore, MD

KEY POINTS

- *TFAP4* mutations are found in >10% of cases of Burkitt lymphoma, a hallmark B-cell malignancy driven by high MYC expression.
- Mechanistically, c-MYC–induced TFAP4 suppresses tumorigenesis of B cells by limiting self-renewal and promoting differentiation.

The proliferative burst of B lymphocytes is essential for antigen receptor repertoire diversification during the development and selective expansion of antigen-specific clones during immune responses. High proliferative activity inevitably promotes oncogenesis, the risk of which is further elevated in B lymphocytes by endogenous gene rearrangement and somatic mutations. However, B-cell–derived cancers are rare, perhaps owing to putative intrinsic tumor-suppressive mechanisms. We show that c-MYC facilitates B-cell proliferation as a protumorigenic driver and unexpectedly coengages counteracting tumor suppression through its downstream factor TFAP4. *TFAP4* is mutated in human lymphoid malignancies, particularly in >10% of Burkitt lymphomas, and reduced TFAP4 expression was associated with poor survival of patients with MYC-high B-cell acute lymphoblastic leukemia. In mice, insufficient TFAP4 expression accelerated c-MYC–driven transformation of B cells. Mechanistically, c-MYC suppresses the stemness of developing B cells by inducing TFAP4 and restricting self-renewal of proliferating B cells. Thus, the pursuant transcription factor cascade functions as a tumor suppressor module that safeguards against the transformation of developing B cells.

Introduction

Lymphocytes are one of the most rapidly proliferating cell types in the postnatal organism.[1–6] Extensive proliferative burst is essential to form diverse antigen receptor repertoires and facilitate requisite antigen-specific immune responses. In addition to demands for accurate DNA replication during extensive cell division, B lymphocytes are vulnerable to genomic instability as a result of DNA editing by recombination-activating gene (RAG) or activation-induced cytidine deaminase that primarily targets antigen receptor loci but also attacks other sites throughout the genome,[7] potentially rendering lymphocytes highly cancer prone. However, cancers derived from developing lymphocytes are rarer than would be expected from their inherent risk, and their incidence is lower than that of common epithelial cancers (eg, 1.7 cases of acute lymphoblastic leukemia [ALL] per 100 000 population annually vs 38-127 cases of colon, lung, and breast cancer per 100 000 population annually).[8] Accordingly, we hypothesized that lymphocytes are protected from transformation by putative tumor-suppressive programs that are tightly linked to their proliferative program. Such programs may preserve the genomic integrity or restrict specific gene-expression programs that would enhance transformation.

The transcription factor c-MYC is a strong oncogenic driver; activating mutations and translocations that deregulate its expression are hallmark features of numerous tumors in humans and mice.[9–11] c-MYC is also essential for the proliferation of normal lymphocytes through control of the cell cycle and metabolism.[12–15] If lymphocytes activate putative tumor suppressors tied to their proliferation, c-MYC itself may directly induce such tumor suppressor genes as a feedback pathway. Therefore, it is conceivable that perturbation of any such pathways might accelerate the development of lymphoid malignancies induced by aberrant c-MYC expression, although it remains unknown whether such a c-MYC–induced tumor-suppressive mechanism exists.

In this study, we profiled direct c-MYC target genes that are mutated in primary human lymphoid cancers and identified the transcription factor TFAP4 (also known as AP4) as a c-MYC–inducible tumor suppressor in B lymphocytes. Recurrent mutations of *TFAP4* are found predominantly in its DNA binding domain in human cancers, including ALL, and a notable proportion of cases of Burkitt lymphoma (BL). In c-MYC–driven mouse B-cell tumor models, TFAP4 functions as a c-MYC–induced haploinsufficient tumor suppressor. Single allele deletion of

Tfap4 or specific deletion of a c-MYC binding site in the locus shortened the latency of the MYC transgene-driven tumorigenesis, with frequent loss of heterozygosity (LOH). Mechanistically, c-MYC drives the proliferation of B-cell progenitors, as well as promotes their differentiation, thus restricting the self-renewing capacity of B cells in undifferentiated states through TFAP4-dependent repression of the stemness factor *Erg*. Finally, reduced expression of *TFAP4*, despite high *c-MYC* expression, is associated with poor prognosis of a subset of patients with B-cell ALL (B-ALL). These results collectively show that the c-MYC–TFAP4 axis has dual roles in supporting the clonal expansion of normal lymphocytes[16,17] and paradoxically, suppresses the transformation of proliferating B cells.

Methods

Mice

Tfap4$^{-/-}$,[18] *Tfap4*$^{F/F}$,[16] *Erg*$^{F/F}$,[19] *Cd79a*-icre,[20] and *Myc*-GFP[21] mice were described previously and were backcrossed to the C57BL/6N background for >10 generations. Eμ-*Myc*,[22] *Ighg1*-cre,[23] *Rosa26*$^{CAG\text{-}MYC}$,[24] and *Rosa26*^{Pik3ca*}[25] mice were from The Jackson Laboratory. C57BL/6N and B6-Ly5.1 mice were from Charles River. All mouse experiments were conducted according to the protocol approved by the Washington University Animal Studies Committee.

Tumorigenesis studies

Eμ-*Myc* mice were monitored weekly for palpable tumor development and body weight loss. Mice were euthanized when tumor sizes exceeded 20 mm in diameter or mice exhibited >20% body weight loss or paralysis. For transplantation of retrovirally transduced B cells, CD19$^+$ bone marrow (BM) cells, isolated using anti-CD19 MicroBeads (Miltenyi Biotec) from 6- to 10-week-old mice, were infected with viral supernatants, followed by IV transfer of 1×10^6 cells into sublethally irradiated (5.5 Gy) mice. For in vivo persistence analysis, transduced cells were transferred into congenic mice at an ~1:1 ratio of *Tfap4*$^{+/-}$, *Tfap4*$^{+/-}$*Erg*$^{+/-}$, or *Erg*$^{+/-}$ cells to wild-type (WT) cells.

Human BL and TARGET data analysis

Gene expression data from BL samples[26] were downloaded from the European Genome-Phenome Archive (EGAS00001003778). Data were analyzed using Galaxy as follows: counts per gene for each sample were obtained by running featureCounts on GRCh38-aligned BAM files and normalized using DESeq2. The normalized data were imported into the Phantasus application[27] for further analysis. After $\log_2$ transformation and quantile normalization, ENTREZ-annotated genes were filtered for mean normalized counts >2 across samples. Data for B-ALL samples were downloaded from TARGET phase II, and gene expression was analyzed in Phantasus. Differentially expressed genes (DEGs) in both patient cohorts were analyzed using a limma tool, followed by gene set enrichment analysis (GSEA).

Statistical analysis

Survival data were compared using the log-rank test with adjustment for multiple comparisons when necessary. *P* values were calculated using an unpaired 2-tailed Student *t* test for 2-group comparisons and 1-way analysis of variance (ANOVA) for multigroup comparisons with the Tukey post hoc test or Kruskal-Wallis test with Dunn's multiple comparison test. Human microarray data from previously published studies were compared using Mann-Whitney's *U* test for 2-group comparisons and the Kruskal-Wallis test for multigroup comparisons. All statistical analyses were done using Prism. Adjusted values of $P < .05$ were considered significant.

Results

The c-MYC downstream transcription factor TFAP4 is mutated in primary human cancers

To determine whether c-MYC engages tumor-suppressive programs in B lymphocytes, we initially defined c-MYC–dependent genes in developing B cells between Eμ-*Myc* and littermate WT B220$^+$ immunoglobulin M (IgM)$^-$ pro/pre-B cells. We combined this analysis with gene expression profiles of mouse germinal center B (GCB) cells[13] and identified 107 genes that were commonly dependent on c-MYC in pro/pre-B and GCB cells (Figure 1A-C). The candidate genes were prioritized based on known roles in gene regulation, direct c-MYC targets,[16,17,28] and mutation frequencies in human hematopoietic malignancies using the COSMIC (Catalogue of Somatic Mutations In Cancer) database. *Tfap4*, encoding a bHLH transcription factor, was identified as a gene meeting all of the criteria (Figure 1D). We confirmed that TFAP4 expression was increased in B220$^+$ IgM$^-$ BM cells from Eμ-*Myc* mice compared with those from littermate WT mice (Figure 1E).

Somatic mutations of *TFAP4* were found in lymphoid and other cancers registered in COSMIC, TCGA (The Cancer Genome Atlas), and PeCan (Pediatric Cancer Genomic Data Portal). Notably, 5 of 6 PeCan cases with *TFAP4* mutations were found in lymphoid tumors (3 BL, 1 B-ALL, and 1 T-cell ALL [T-ALL]). Although *TFAP4* mutations in these databases were rare (288/37 420 unique samples in COSMIC, 65/10 202 in TCGA, and 6/2578 in PeCan), analyses identified missense *TFAP4* mutations in 12 of 101 cases in the BL data set:[26] 6 of 32 endemic BLs and 6 of 69 sporadic and HIV$^+$ cases (Figure 1F; supplemental Figure 1A-B, available on the *Blood* Web site). Across these data sets, the majority of recurrent somatic mutations (≥4 independent cases), including 4 of 6 cases in PeCan lymphoid tumors and 3 additional BL cases, were mapped to the DNA binding domain (basic region)[29] (Figure 1G-H). A single amino acid substitution in the DNA binding residue was sufficient to compromise its transactivating potential, because expression of CD25/*Il2ra*, a direct TFAP4 target gene, was reduced in *Tfap4*$^{-/-}$ CD8 T cells retrovirally complemented with the R50W or R60H variant compared with WT-TFAP4 or the R129W variant harboring a mutation outside of the basic region (Figure 1I; supplemental Figure 1C-F). These results suggest that the somatic mutations found in the basic region impair TFAP4 function and that the dysfunction of TFAP4 contributes to oncogenesis in lymphoid malignancies.

TFAP4 is a cell-intrinsic tumor suppressor

Because *Tfap4* is a c-MYC–inducible gene[16,17,30] and many tumors associated with *TFAP4* mutations express high levels of c-MYC, we next determined whether TFAP4 modulates c-MYC–induced tumorigenesis in B cells. We first used the Eμ-*Myc* mouse model, in which *Myc* is expressed under the control of the *Igh* μ enhancer, mimicking the t(8;14) *IGH-MYC* translocation.[22] In this model, c-MYC is overexpressed in developing B cells

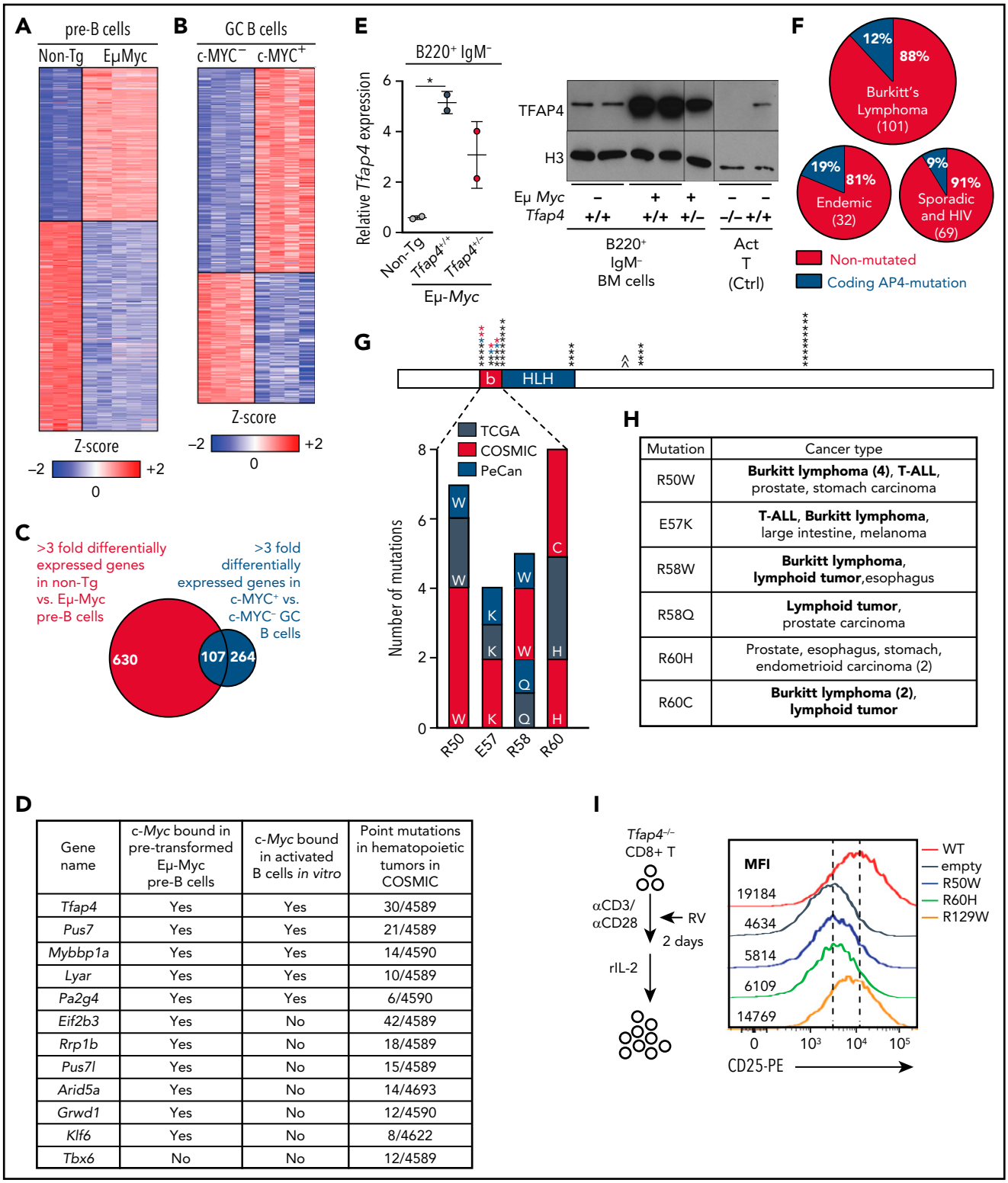

H

Mutation	Cancer type
R50W	**Burkitt lymphoma (4)**, **T-ALL**, prostate, stomach carcinoma
E57K	**T-ALL**, **Burkitt lymphoma**, large intestine, melanoma
R58W	**Burkitt lymphoma**, **lymphoid tumor**,esophagus
R58Q	**Lymphoid tumor**, prostate carcinoma
R60H	Prostate, esophagus, stomach, endometrioid carcinoma (2)
R60C	**Burkitt lymphoma (2)**, **lymphoid tumor**

D

Gene name	*c-Myc* bound in pre-transformed Eμ-Myc pre-B cells	*c-Myc* bound in activated B cells *in vitro*	Point mutations in hematopoietic tumors in COSMIC
Tfap4	Yes	Yes	30/4589
Pus7	Yes	Yes	21/4589
Mybbp1a	Yes	Yes	14/4590
Lyar	Yes	Yes	10/4589
Pa2g4	Yes	Yes	6/4590
Eif2b3	Yes	No	42/4589
Rrp1b	Yes	No	18/4589
Pus7l	Yes	No	15/4589
Arid5a	Yes	No	14/4693
Grwd1	Yes	No	12/4590
Klf6	Yes	No	8/4622
Tbx6	No	No	12/4589

Figure 1. The transcription factor TFAP4 is induced by MYC in developing B cells and GCB cells and is mutated in lymphoid cancers. (A) Z score heat map showing expression of genes that are differentially expressed at least threefold by pro/pre-B cells from Eμ-*Myc*$^{-}$ *Tfap4*$^{+/+}$ (non-Tg; n = 3) and Eμ-*Myc* *Tfap4*$^{+/+}$ (n = 5) mice, as determined by RNA sequencing. (B) Z score heat map showing expression of genes that are differentially expressed at least threefold by c-MYC^{+} vs c-MYC^{-} mouse splenic GCB cells, as determined by microarray (GSE38304). (C) Overlap of DEGs in (A) and (B). (D) Overlapping genes from panel C involved in gene regulation with direct c-MYC binding to each genomic region and mutation frequencies in hematopoietic tumors in COSMIC. The list is sorted by the numbers of point mutations in hematopoietic tumors after prioritization of c-MYC–bound genes. (E) Quantitative reverse transcription polymerase chain reaction (left panel) and immunoblot analysis (right panel) of *Tfap4* mRNA and TFAP4 protein in BM B220^{+} IgM^{-} cells of Eμ-*Myc*$^{-}$ *Tfap4*$^{+/+}$ (non-Tg) and Eμ-*Myc*$^{+}$ *Tfap4*$^{+/+}$ and *Tfap4*$^{+/-}$ mice. *Tfap4* mRNA expression was normalized to spike-in control RNA, ERCC-00108. Histone H3 serves as a loading control in immunoblot. (F) Frequency of coding *TFAP4* mutations registered across BL subtypes.[26] (G) Mapping of recurrent (≥4 independent) somatic missense mutations of *TFAP4* identified in primary human tumors from TCGA, PeCan, and COSMIC

starting at the pro-B–cell stage, leading to B-cell malignancy and nearly all mice dying within a year (Figure 2A). In striking contrast, haploinsufficiency of *Tfap4* in Eμ-*Myc* mice accelerated tumorigenesis, with all mice dying by day 92, whereas homozygous *Tfap4* deletion further accelerated tumorigenesis (Figure 2A). In 40% of tumors in Eμ-*Myc* mice, B220^{+} cells exhibited an immature phenotype, expressing *Rag1* and *VpreB1* (Figure 2B; supplemental Figure 2A-B), consistent with previous studies.[31,32] In contrast, 93% of Eμ-*Myc Tfap4*$^{+/-}$ mice formed tumors with the immature phenotype (Figure 2B). The skewing of tumors toward the immature phenotype suggests that pro/pre-B cells with elevated c-MYC, but reduced TFAP4, become transformed with shorter latency after c-MYC is turned on in pro-B cells. The numbers of developing B cells, their short-term proliferation, and annexin V binding at the population level were comparable between *Tfap4*-haploinsufficient and *Tfap4*-proficient Eμ-*Myc* mice before tumor formation (supplemental Figure 2C-F). No survival difference was observed between *Tfap4*$^{+/+}$ and *Tfap4*$^{+/-}$ Eμ-*Myc* pro/pre-B cells ex vivo (supplemental Figure 2G-H).

To determine whether TFAP4-mediated supression of Eμ-*Myc* tumors is cell-intrinsic, we deleted 1 or 2 *Tfap4*^{F} alleles in pro-B cells using *Cd79a*^{icre}, recapitulating the accelerated tumorigenesis and immunophenotype observed in germline *Tfap4*-deficient mice (Figure 2C; supplemental Figure 2I). We also tested whether TFAP4 functions as a suppressor of c-MYC–induced B cell malignancies in additional mouse models, because almost all B cells express aberrant MYC throughout their development in Eμ-*Myc* mice. First, we retrovirally expressed c-MYC in CD19^{+} BM cells from *Tfap4*$^{-/-}$ or *Tfap4*$^{+/+}$ mice, followed by transfer to sublethally irradiated mice. In this model, we typically achieve transduction of ∼10% of pro/pre-B cells (data not shown), and tumor formation by c-MYC–transduced pre-B cells is dependent on a defect in a tumor suppressor.[33,34] In contrast to control mice receiving c-MYC–transduced *Tfap4*$^{+/+}$ CD19^{+} cells, the majority of mice receiving c-MYC–transduced *Tfap4*$^{-/-}$ CD19^{+} BM cells died from pre-B–cell tumors (Figure 2D; supplemental Figure 2J). We also observed accelerated B-ALL disease progression induced by ectopic expression of p190 *bcr-abl*, which indirectly upregulates *Myc*, in CD19^{+} BM cells from *Tfap4*$^{-/-}$ mice compared with those from *Tfap4*$^{+/+}$ mice (Figure 2E; supplemental Figure 2K). In addition to these immature B-cell malignancies, we observed accelerated death in the absence of TFAP4 in a mature B-cell lymphoma model induced by c-MYC and a constitutively active phosphatidylinositol 3-kinase[24] (Figure 2F). These data establish a cell-intrinsic requirement for TFAP4 in the suppression of MYC-mediated B-cell cancers in multiple mouse models.

c-MYC bound 2 consensus sites within the H3K27ac-marked intronic region at the *Tfap4* locus in Eμ-*Myc* B220^{+} BM cells (supplemental Figure 3A). To determine whether direct activation of *Tfap4* by c-MYC binding to this enhancer is necessary for tumor suppression, we deleted a 1-kb intronic region containing the 2 consensus sites using CRISPR/Cas9 (supplemental Figure 3A). Heterozygous deletion of the 1-kb region in Eμ-*Myc* mice recapitulated accelerated tumorigenesis (supplemental Figure 3B-C). This might be caused by the loss of other transcription factors binding at the enhancer or indirectly by altered expression of the neighboring genes. However, a more specific single-allele deletion of 1 MYC binding site also shortened survival of these mice compared with Eμ-*Myc* mice harboring WT *Tfap4* loci (supplemental Figure 3B), whereas expression of 2 genes around the *Tfap4* locus, or *Runx1* located on the same chromosome, was unaffected (supplemental Figure 3C). Thus, direct activation of *Tfap4* by c-MYC is essential for tumor suppression.

LOH of TFAP4 confers interclonal competitiveness for tumor outgrowth

Tfap4 messenger RNA (mRNA) expression was comparable between pro/pre-B cells before transformation and pro/pre-B tumor cells in Eμ-*Myc Tfap4*$^{+/+}$ mice (Figure 3A). However, approximately one third of pro/pre-B tumors from Eμ-*Myc Tfap4*$^{+/-}$ mice expressed substantially lower *Tfap4* mRNA compared with pretransformed pro/pre-B cells (Figure 3A, dashed rectangle). This reduced *Tfap4* expression was caused by LOH in these tumors (Figure 3B). A genomic region encompassing exons 2 through 4, deleted in the *Tfap4*$^{-}$ allele, was detectable in all tumors from Eμ-*Myc Tfap4*$^{+/+}$ mice and a subset of tumors from Eμ-*Myc Tfap4*$^{+/-}$ mice. By contrast, this genomic region was lost in tumor cells with low *Tfap4* expression from Eμ-*Myc Tfap4*$^{+/-}$ mice (Figure 3B, dashed rectangle). LOH of *Tfap4* was also confirmed by loss of mCherry (mC) fluorescence in Eμ-*Myc* tumors harboring 1 null and 1 functional TFAP4-mC fusion knock-in allele[17] (*Tfap4*$^{mC/-}$) (Figure 3C-D). These results indicate that, although TFAP4 downregulation is unnecessary for transformation, rare clones undergoing LOH at the *Tfap4* locus predominantly contribute to tumorigenesis.

A c-MYC target gene signature is commonly enriched in Eμ-*Myc Tfap4*$^{+/-}$ tumors and TFAP4-mutated BL in humans

To gain insights into the molecular mechanisms of c-MYC–TFAP4–dependent tumor suppression, we profiled the gene expression of pretransformed B220^{+} IgM^{-} pro/pre-B cells, validated by unbiased expression of *Ighv* transcripts (supplemental Figure 4A), from Eμ-*Myc Tfap4*$^{+/-}$ mice and control Eμ-*Myc Tfap4*$^{+/+}$ mice at 3 to 4 weeks of age. Because of rapid tumor development, analysis of pretransformed Eμ-*Myc Tfap4*$^{-/-}$ pro/pre-B cells was excluded. Gross transcriptomic differences determined by principal component analysis and the expression of genes related to apoptosis, proliferation, and senescence were not detected between Eμ-*Myc Tfap4*$^{+/-}$ cells and Eμ-*Myc Tfap4*$^{+/+}$ cells (supplemental Figure 4B-D). At the gene level, 29 genes were differentially expressed by ≥1.8-fold. Among these, 20 genes were directly bound by TFAP4, as confirmed by chromatin immunoprecipitation sequencing (current study), and 9 of the 20 genes were shared TFAP4 and MYC targets[28] in Eμ-*Myc* B cells (Figure 4A-C). Despite the lack of clear genotype-associated clustering (supplemental Figure 4E), an expression

Figure 1. (continued) databases. Each mutation is shown by an asterisk and is mapped to its position in the TFAP4 protein; PeCan lymphoid tumors are shown in blue, and Duke BL cases are shown in red. The basic region (b) functioning as a DNA binding domain and the helix-loop-helix (HLH) domain are shown. A caret (^) indicates that the R129W mutation is found outside of this region. (H) List of recurrent somatic mutations in the DNA binding region and their cancer types in panel G with hematopoietic malignancies shown in bold. (I) Assay to determine the function of somatic TFAP4 variants in upregulation of CD25, which is a direct TFAP4 target (supplemental Figure 1C-E), in *Tfap4*$^{-/-}$ CD8 T cells (left panel). Expression of CD25 in *Tfap4*$^{-/-}$ CD8 T cells retrovirally expressing each TFAP4 somatic variant (right panel). Data are representative of 3 independent experiments . *$P < .05$ by 1-way ANOVA. Ctrl, control; MFI, median fluorescence intensity; rIL-2, recombinant interleukin-2; RV; retrovirus; α, anti-.

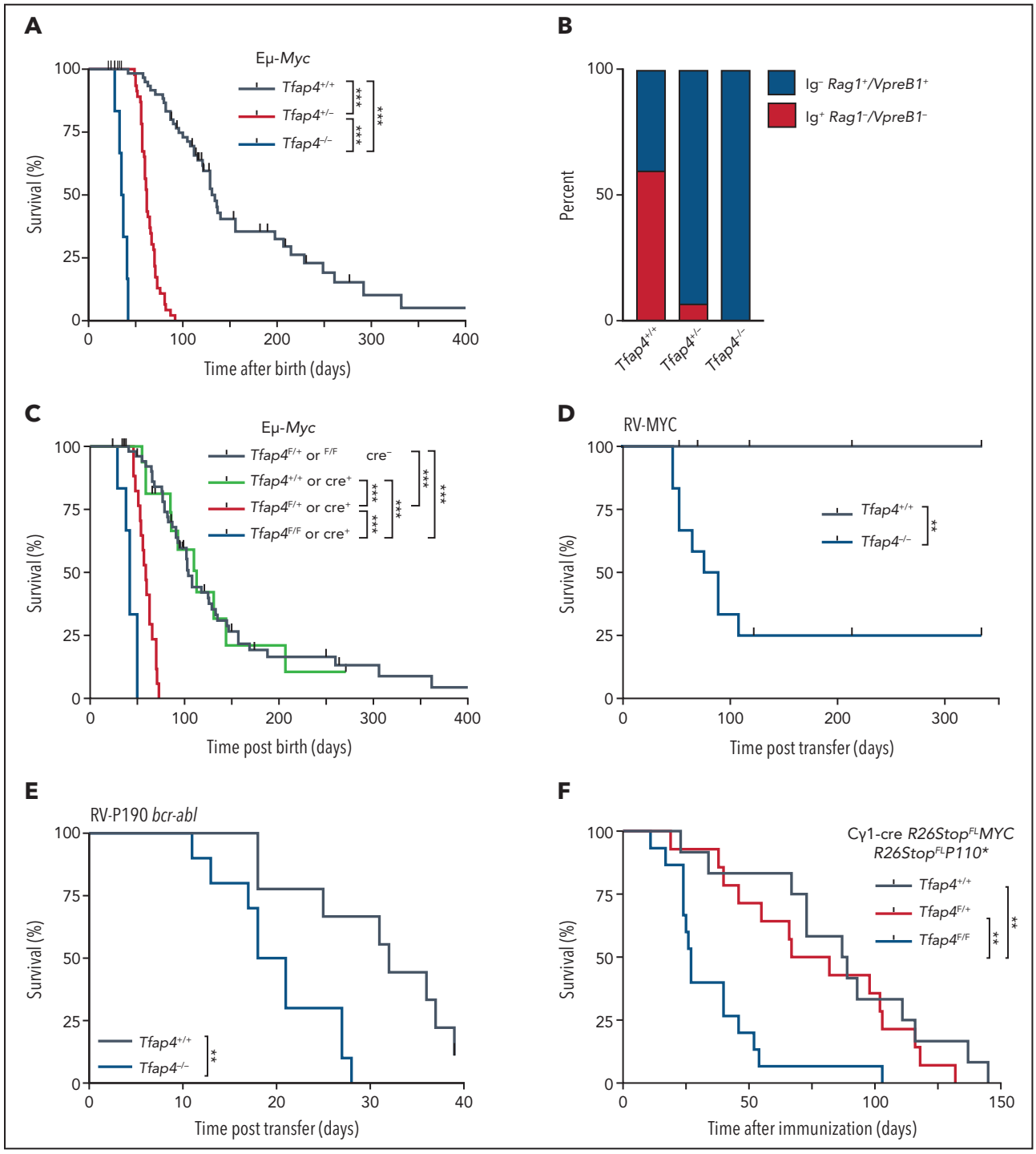

Figure 2. TFAP4 is a c-MYC–induced cell-intrinsic tumor suppressor in developing B cells. (A) Survival analysis of Eμ-*Myc* mice crossed to *Tfap4*$^{+/+}$ mice (n = 68), *Tfap4*$^{+/-}$ mice (n = 50), or *Tfap4*$^{-/-}$ mice (n = 6). The median survival was 134, 62, and 36 days, respectively. (B) Frequencies of surface Ig^{-} *Rag1*$^{+}$ *VpreB1*$^{+}$ (immature) and Ig^{+} *Rag1*$^{-}$ *VpreB1*$^{-}$ (mature) B-cell tumors in Eμ-*Myc* mice with distinct *Tfap4* genotypes (Eμ-*Myc* *Tfap4*$^{+/+}$, n = 10; Eμ-*Myc* *Tfap4*$^{+/-}$, n = 14; Eμ-*Myc* *Tfap4*$^{-/-}$, n = 2). (C) Survival of Eμ-*Myc* mice with *Cd79ai*^{cre}–mediated deletion of the *Tfap4* allele in developing B cells (*Tfap4*$^{F/+}$ or *Tfap4*$^{F/F}$ cre^{-} [n = 59], median survival, 104 days; *Tfap4*$^{+/+}$ *Cd79a*$^{icre/+}$ [n = 16], median survival, 113 days; *Tfap4*$^{F/+}$ *Cd79a*$^{icre/+}$ [n = 17], median survival, 59 days; *Tfap4*$^{F/F}$ *Cd79a*$^{icre/+}$ [n = 6], median survival, 42 days). (D) Tumorigenesis of *Tfap4*$^{+/+}$ or *Tfap4*$^{-/-}$ BM CD19^{+} cells retrovirally transduced with mouse c-MYC (T58A) and adoptively transferred into sublethally irradiated CD45.1 mice (*Tfap4*$^{+/+}$ [n = 10], median survival, undefined days; *Tfap4*$^{-/-}$ [n = 12], median survival, 83.5 days;). Two independent experiments were combined. (E) Survival of mice receiving *Tfap4*$^{+/+}$ or *Tfap4*$^{-/-}$ BM CD19^{+} cells transduced with human P190 *bcr-abl*–expressing retrovirus and adoptively transferred into sublethally irradiated CD45.1 mice (*Tfap4*$^{+/+}$ [n = 9], median survival, 32 days; *Tfap4*$^{-/-}$ [n = 10], median survival, 19.5 days). Two independent experiments were combined. (F) Survival of lethally irradiated CD45.1 mice reconstituted with BM cells from Cγ1-cre *R26Stop*$^{LSL\text{-}MYC}$ × *R26Stop*$^{LSL\text{-}P110*}$ mice of the indicated *Tfap4* genotypes following immunization with sheep red blood cells. Data are combined from 4 independent experiments. *Tfap4*$^{+/+}$ (n = 12), median survival, 88 days; *Tfap4*$^{F/+}$ (n = 14), median survival, 74.5 days; *Tfap4*$^{F/F}$ (n = 15), median survival: 27 days. $^{**}P < .01$, $^{***}P < .001$, log-rank test adjusted for multiple comparisons. RV, retrovirus.

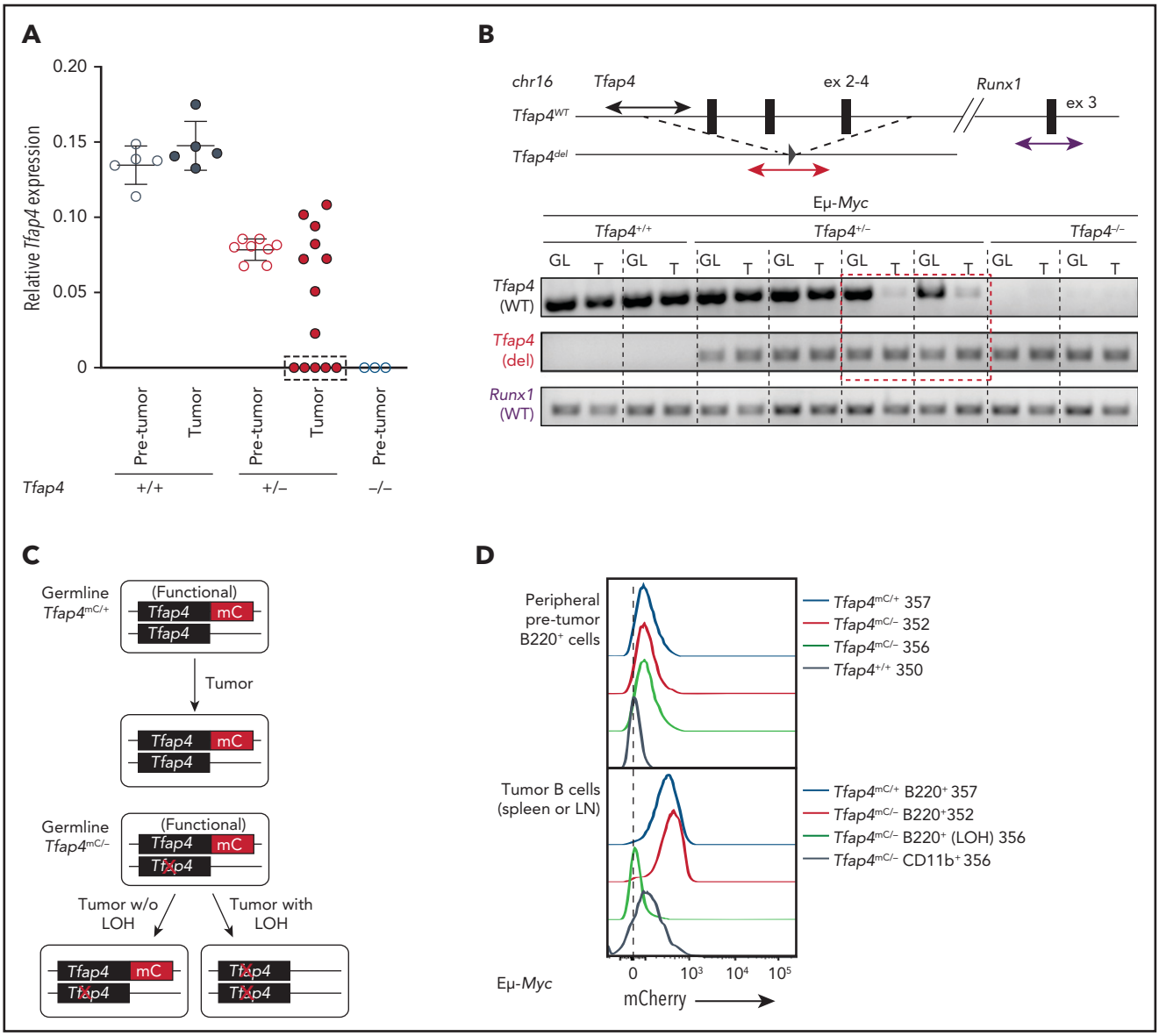

Figure 3. Low levels of TFAP4 endow interclonal competition of pretransformed B-cell precursors with aberrant c-MYC expression. (A) Expression of *Tfap4* mRNA in pretransformed B220$^+$IgM$^-$ BM (Pre-tumor) or B220$^+$ IgM$^-$ tumor (Tumor) cells harvested from Eμ-*Myc* mice with the indicated *Tfap4* genotypes. *Tfap4* mRNA expression, measured by quantitative reverse transcription polymerase chain reaction (PCR), was normalized to *Hprt1* expression. (B) Genomic PCR detecting the region of the *Tfap4* allele encompassing exons 2-4 in tumor DNA (T) and tail DNA (GL, germline) of each corresponding mouse. A genomic region containing *Runx1* located on the same chromosome was used as an internal control. Three of 5 lymphomas with low *Tfap4* mRNA expression were analyzed by genomic PCR; the red dashed box indicates 2 representative samples with LOH of *Tfap4* in tumors. (C) Diagram showing the detection of LOH using *Tfap4*-mC reporter knock-in mice. (D) Detection of TFAP4-mC fusion protein in peripheral blood B cells from healthy 4-week old Eμ-*Myc Tfap4*$^{mC/+}$ and Eμ-*Myc Tfap4*$^{mC/-}$ mice (upper panel). Loss of TFAP4-mC expression in Eμ-*Myc Tfap4*$^{mC/-}$ tumor B cells with LOH or CD11b$^+$ cells as internal mC$^-$ control (lower panel). The numbers to the right represent unique mouse IDs. chr16, chromosome 16; ex, exon; w/o, without.

pattern of 17 of these 29 genes was preserved in *Tfap4*-deficient tumors, suggesting that their expression is maintained, or selected for, during tumorigenesis (supplemental Figure 4F).

To further examine gene expression program modules that were altered specifically in *Tfap4*-deficient pre-B tumors compared with *Tfap4*-proficient pre-B tumors, we conducted GSEA. Among curated gene sets in the Molecular Signature Database (https://www.gsea-msigdb.org/gsea/msigdb/),[35–37] genes related to MYC targets and E2F targets were significantly enriched in *Tfap4*-deficient/haploinsufficient tumors (Figure 4D-E). Gene sets associated with MYC and E2F targets were also significantly enriched in human BL samples harboring somatic *TFAP4* mutations (Figure 4D-E). These findings suggest that TFAP4 functions as a negative feedback factor that restricts proliferative states of tumorigenic cells associated with high c-MYC and E2F activity. Unsupervised clustering of DEGs in pre-B–cell tumors with distinct *Tfap4* genotypes revealed 2 clusters specifically associated with reduced *Tfap4* expression (Figure 4F, clusters II/III). These clusters were enriched for genes associated with cancer/p53-related pathways (supplemental Figure 4H). In addition, a gene signature associated with an upregulated KRAS signaling pathway, which has been associated with the Eμ-*Myc* model,[38–40] was enriched specifically in Eμ-*Myc Tfap4*$^{+/-}$ tumors (Figure 4F, cluster VIII; supplemental

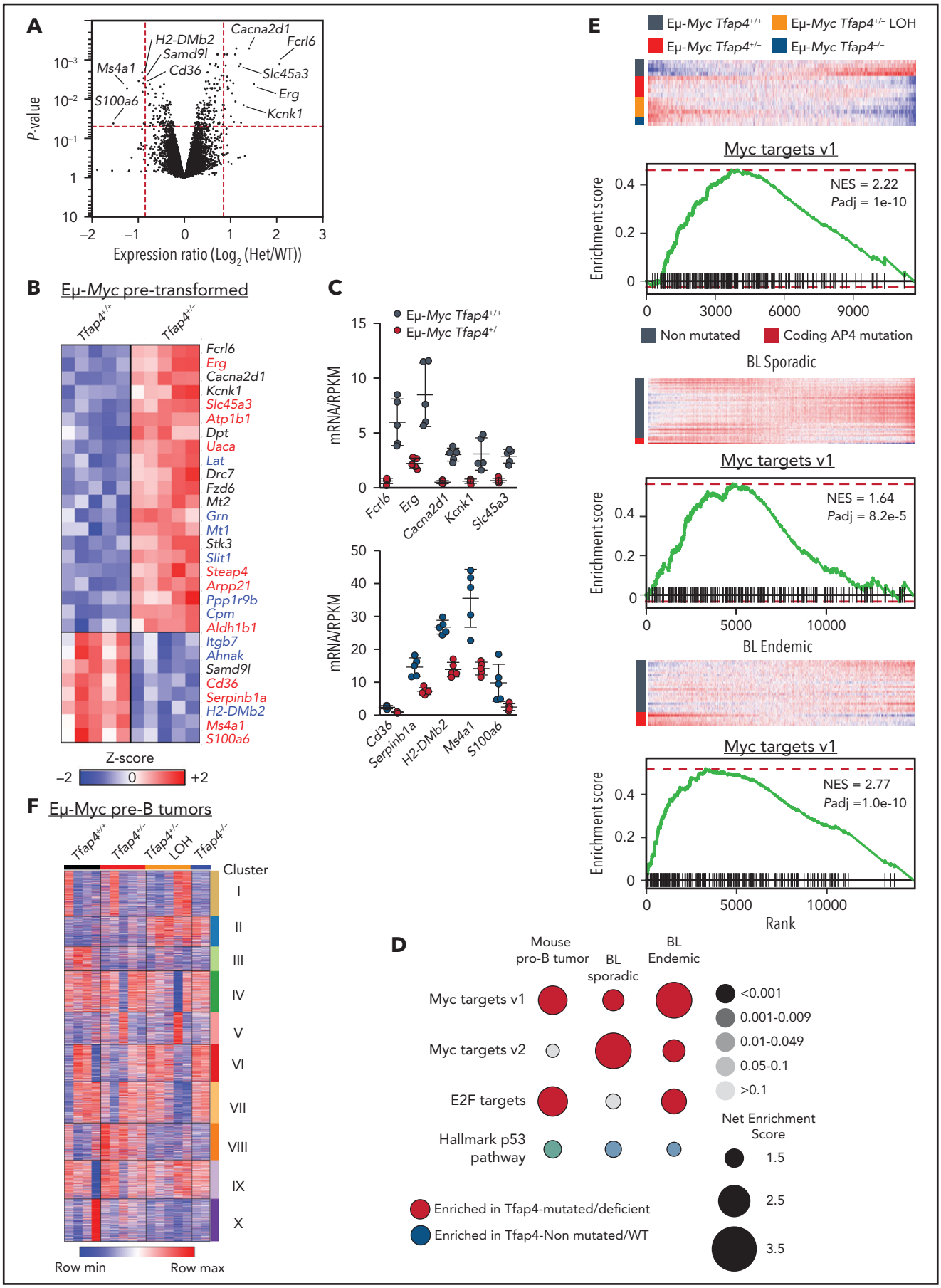

Figure 4.

Figure 4H). Consistently, whole-exome sequencing and targeted sequencing of the tumor samples, which were mostly clonal or oligoclonal (supplemental Figure 5A), revealed frequent *Kras* mutations in Eμ-*Myc Tfap4*$^{+/-}$ tumors, despite similar overall mutational burdens (supplemental Figure 5B-D). Overall, transcriptomic and genetic data suggest that TFAP4-dependent tumor suppression is mediated by the regulation of persistent engagement of cell proliferation via specific gene pathways rather than protection against global genomic instability.

Restriction of the proto-oncogene *Erg* is required for tumor suppression by TFAP4

TFAP4 supports the continued proliferation of normal lymphocytes by supplementing an early decay of c-MYC by maintaining the expression of numerous c-MYC target genes, but it is dispensable when c-MYC is expressed.[16,17] However, during tumorigenesis, our data showed that TFAP4 counteracts c-MYC–mediated transformation of developing B cells, likely through control of its unique targets. Among the unique TFAP4 targets in Figure 4B, *Erg*, encoding an ETS-family transcription factor, has been implicated in hematopoietic malignancies. *Erg* is also necessary to maintain the stemness of hematopoietic stem cells (HSCs).[41] ERG overexpression in mouse hematopoietic progenitor cells causes lymphoid and megakaryocytic cancers.[42–45] In humans, although impaired ERG function has been associated with a small subset of B-ALL specifically harboring a DUX4 rearrangement,[45,46] *ERG* was overexpressed in a majority of B-ALL cases compared with other tumor types and normal BM cells across multiple studies[47–51] (supplemental Figure 6A-E). Despite the limited sample number with gene expression data available, a human T-ALL case with a TFAP4^{E57K} substitution and an *LMO2-LYL1* translocation in PeCan expressed *ERG* at a level higher than the 95% confidence interval of *ERG* expression in other T-ALL samples with an *LMO2-LYL1* or *LMO1-LMO2* translocation (supplemental Figure 6F-G), suggesting that elevated *ERG* is associated with functionally defective TFAP4.

In Eμ-*Myc Tfap4*$^{+/-}$ pretransformed pro/pre-B cells, *Erg* expression was elevated by 3.8-fold compared with controls (Figure 5A). *Erg* was further upregulated in pro/pre-B tumors lacking TFAP4 (Figure 5B). TFAP4 bound an intronic region of the *Erg* locus, colocalizing with H3K27ac-marked accessible chromatin in Eμ-*Myc* B cells, whereas c-MYC binding was not detected in the genomic region encompassing the *Erg* locus (Figure 5C). These results suggest that *Erg* is a direct TFAP4 target. *Erg* is coexpressed with *Myc* and *Tfap4* in pro-B cells before the *Igh* checkpoint at the population level but is downregulated in proliferating large pre-B cells as they differentiate into small pre-B cells (Figure 5D). However, within c-kit^{+} pro-B cells, expression of c-MYC protein correlates inversely with that of *Erg* mRNA, with *Erg* expression enriched in c-MYC^{-} pro-B cells and significantly downregulated as cells upregulate c-MYC during the transition to large pre-B cells (Figure 5E). Therefore, we hypothesized that *Erg* must be regulated in c-MYC^{+} B cells in a TFAP4-dependent manner to restrict the risk of tumorigenesis, because c-MYC and ERG are required for B-cell development but are also oncogenic. Accordingly, *Erg* was elevated in *Tfap4*$^{-/-}$ vs *Tfap4*$^{+/+}$ c-MYC^{+} pro-B cells (Figure 5F). Furthermore, TFAP4-mediated *Erg* suppression was even more apparent in Eμ-*Myc* mice, because *Erg* was completely suppressed in Eμ-*Myc* vs WT B220^{+} IgM^{-} cells (Figure 5G). *Erg* suppression was partially reversed and completely lost in Eμ-*Myc Tfap4*$^{+/-}$ and Eμ-*Myc Tfap4*$^{-/-}$ pretransformed pro/pre-B cells, respectively (Figure 5G). These results indicate that TFAP4 prevents simultaneous expression of the 2 proto-oncogenes, c-MYC and ERG, in differentiating B cells.

To directly determine whether *Erg* derepression accelerates tumorigenesis, we deleted one *Erg* allele in Eμ-*Myc Tfap4*$^{+/-}$ mice, because complete loss of *Erg* arrests B-cell development.[52] *Erg* haploinsufficiency significantly delayed tumor onset and extended the survival of Eμ-*Myc Tfap4*$^{+/-}$ mice (Figure 5H). Furthermore, B-cell tumors that developed in *Erg*$^{+/-}$ mice were skewed toward the mature phenotype lacking expression of *Rag1* and *Vpreb1* (Figure 5I), indicating prolonged latency to transformation after MYC was turned on. These results indicate that TFAP4 suppresses the MYC-mediated transformation of B-cell precursors, at least in part, through the regulation of *Erg*.

TFAP4 suppresses tumorigenesis by coupling c-MYC–driven proliferation and differentiation of B-cell progenitors

ERG maintains the undifferentiated state of HSCs by inhibiting c-MYC targets, whereas c-MYC antagonizes self-renewal in favor of differentiation.[41,53] Because our data demonstrated that c-MYC suppresses *Erg* through TFAP4, we hypothesized that TFAP4 prevents B-cell progenitors from maintaining their undifferentiated state or stemness while rapidly proliferating, thus restricting transformation. To test this, we adoptively transferred a mixture of *Tfap4*$^{+/+}$ and *Tfap4*$^{+/-}$ CD19^{+} cells transduced with c-MYC marked by distinct reporters, with comparable infection efficiency across genotypes, into sublethally irradiated congenic mice and assessed their expansion and differentiation (Figure 6A; supplemental Figure 6H). Three weeks after transfer, *Tfap4*$^{+/-}$ cells became dominant among the total transduced donor-derived B220^{+} cells (Figure 6B-C). In addition to superior expansion and persistence of MYC^{+} *Tfap4*$^{+/-}$ cells, frequencies of IgM^{+} cells were significantly lower in *Tfap4*$^{+/-}$ cells compared with *Tfap4*$^{+/+}$ cells (Figure 6D). These results imply that *Tfap4*$^{+/-}$ pro/pre-B cells

Figure 4. Gene expression changes associated with c-MYC target gene signature are enriched in mouse Eμ-*Myc Tfap4*$^{+/-}$ tumors and *TFAP4*-mutated BL patient samples. (A) Volcano plot showing gene expression changes between pretransformed Eμ-*Myc Tfap4*$^{+/+}$ and Eμ-*Myc Tfap4*$^{+/-}$ B220^{+} IgM^{-} BM cells. Log_2-fold change and *P* values were calculated using a *limma* R package through the Phantasus application. Red dashed lines indicate cutoff thresholds for fold-change >1.8 and $P < .05$. The top 5 most DEGs in either direction are labeled. (B) Annotation and z score heat map of genes differentially expressed by >1.8-fold in (A). Genes bound by TFAP4 or cobound by TFAP4 and MYC, as determined by chromatin immunoprecipitation sequencing, are shown in red and blue, respectively. (C) Expression of DEGs, defined in (B), by pretransformed pro/pre-B cells from mice with the indicated *Tfap4* genotypes. Upper panel: upregulated genes; lower panel: downregulated genes. (D) GSEA of *Tfap4*-deficient/mutated vs *Tfap4*-WT/nonmutated mouse tumor B cells or human BL samples relative to the indicated gene set signatures. Dot sizes, colors, and color gradients indicate the net enrichment score, positive or negative enrichment, and adjusted *P* value, respectively. (E) GSEA illustrating the selective upregulation of MYC target genes in *Tfap4*-deficient/haploinsufficient mouse tumors (top panels) and *TFAP4*-mutated human sporadic (middle panels) or endemic (bottom panels) BL samples. (F) K-means clustering (10 clusters) of genes expressed in pro/pre-B tumor cells from Eμ-*Myc* mice with indicated *Tfap4* genotypes. Het, heterozygous; max, maximum; min, minimum; NES, net enrichment score; Padj, adjusted *P* value; RPKM, reads per kilobase of transcript, per million mapped reads.

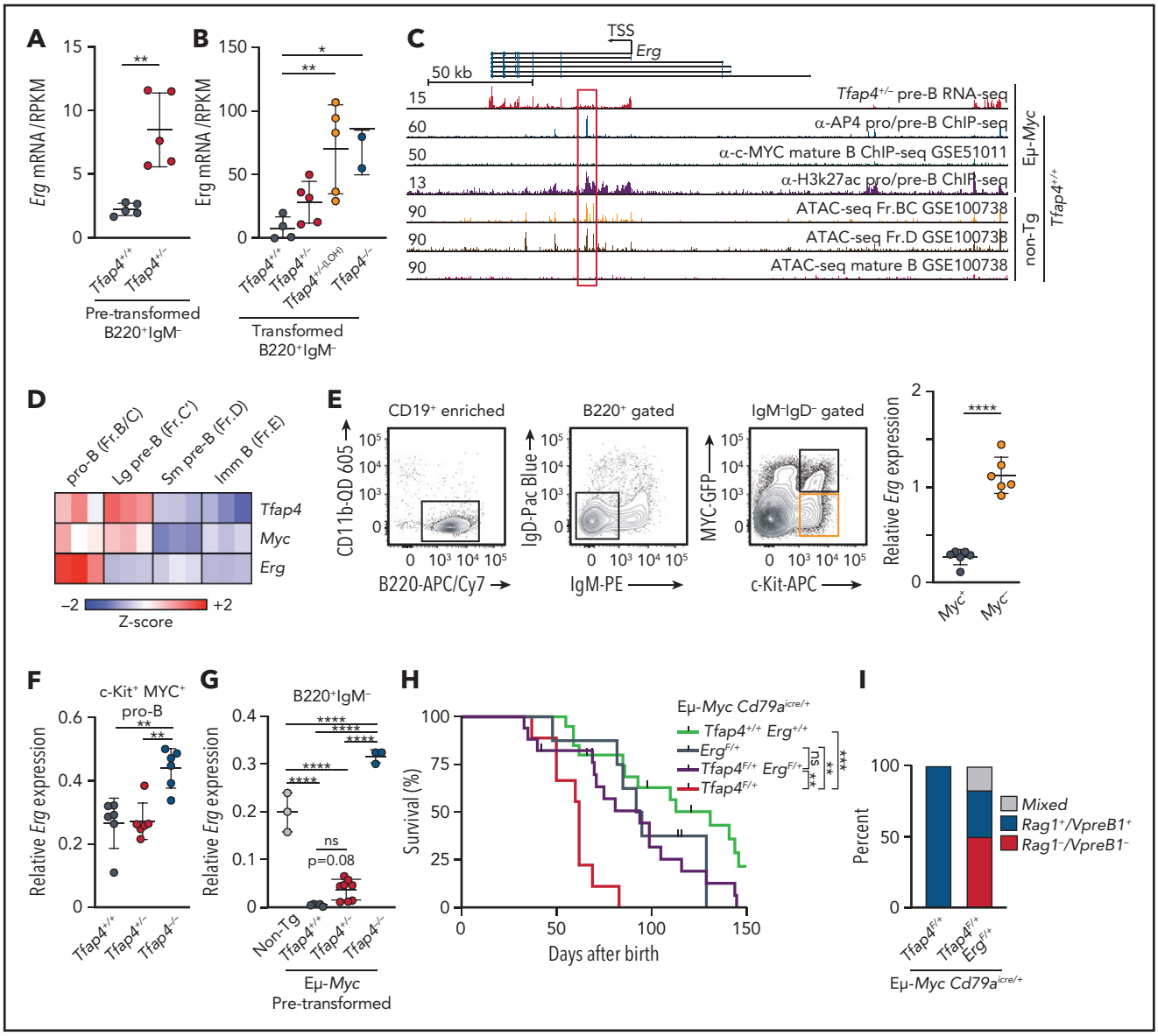

Figure 5. Repression of *Erg* by TFAP4 in MYC$^+$ developing B cells is required for tumor suppression. Expression of *Erg* in pretransformed B220$^+$ IgM$^-$ pro/pre-B cells from Eμ-*Myc Tfap4*$^{+/+}$ mice and Eμ-*Myc Tfap4*$^{+/-}$ mice (A) and pro/pre-B tumor cells from Eμ-*Myc Tfap4*$^{+/+}$, Eμ-*Myc Tfap4*$^{+/-}$, and Eμ-*Myc Tfap4*$^{-/-}$ mice (B), as determined by RNA sequencing. (C) Colocalization of TFAP4 binding and accessible chromatin in the *Erg* locus (red vertical lines indicate exons; black horizontal lines represent introns) in developing B cells, pre-B cells (B220$^+$ IgM$^-$), pro/pre-B cells (CD19$^+$); Fr.BC (CD19$^+$ IgM$^-$ CD43$^+$ CD24$^+$), and Fr.D (CD19$^+$ IgM$^-$ CD43$^-$ B220$^+$). Y-axes show tag counts in 10^7 mapped reads. The Gene Expression Omnibus accession number for each dataset is indicated. (D) Expression of *Tfap4*, *Myc*, and *Erg* mRNA in developing B cells from the Immunological Genome Project database. (E) Sorting strategy for MYC$^+$ and MYC$^-$ pro-B cells in *Myc*$^{+/MYC\text{-}GFP}$ protein reporter mice (far left, near left, and near right panels).[21] Expression of *Erg* mRNA in MYC$^+$ vs MYC$^-$ pro-B cells (far right panel). mRNA expression measured by quantitative reverse transcription polymerase chain reaction was normalized to *Hprt1*. (F) Expression of *Erg* in MYC$^+$ pro-B cells from *Tfap4*$^{+/+}$, *Tfap4*$^{+/-}$, and *Tfap4*$^{-/-}$ mice harboring the MYC-GFP reporter. (G) Expression of *Erg* in CD19$^+$ IgM$^-$ pro/pre-B cells from Eμ-*Myc*$^-$ *Tfap4*$^{+/+}$ (non-Tg), Eμ-*Myc Tfap4*$^{+/+}$, *Tfap4*$^{+/-}$ and *Tfap4*$^{-/-}$ mice prior to tumor development. (H) Survival of *Tfap4*-haploinsufficient Eμ-*Myc* mice with restricted *Erg* expression (*Cd79a*$^{icre/+}$ [n = 20], median survival, 131 days; *Erg*$^{F/+}$ *Cd79a*$^{icre/+}$ [n = 8], median survival, 93.5 days; *Tfap4*$^{F/+}$ *Erg*$^{F/+}$ *Cd79a*$^{icre/+}$ [n = 17], median survival, 94 days; *Tfap4*$^{F/+}$ *Cd79a*$^{icre/+}$ [n = 9], median survival, 62 days). (I) Frequencies of immature (*Rag1* and/or *VpreB1*–expressing and surface Ig$^-$) and mature (*Rag1* and *VpreB1*–nonexpressing and surface Ig$^-$ or Ig$^+$) B-cell tumors in Eμ-*Myc* mice with the indicated genotypes (Eμ-*Myc Tfap4*$^{F/+}$ *Cd79a*$^{icre/+}$, n = 3; Eμ-*Myc Tfap4*$^{F/+}$ *Erg*$^{F/+}$ *Cd79a*^{icre}, n = 6). *P < .05, **P < .01, ***P < .001, ****P < .0001, unpaired *t* test (A,E), one-way ANOVA with Tukey's post hoc test (B,F-G), log-rank test, adjusted for multiple comparisons (H). ATAC-seq, assay for transposase-accessible chromatin with sequencing; ChIP-seq, chromatin immunoprecipitation sequencing; Fr., fraction; Imm, immature; Lg, large; ns, no statistical significance; RNA-seq, RNA sequencing; RPKM, reads per kilobase of transcript, per million mapped reads; Sm, small; TSS, transcription start site; α-, anti-.

maintain their undifferentiated state during c-MYC–driven proliferation as a result of high *Erg* expression. Indeed, reducing *Erg* expression to 50% in *Tfap4*$^{+/-}$ pro/pre-B cells diminished the expansion of overall donor-derived cells, primarily as a result of the reduced expansion of *Tfap4*$^{+/-}$ cells relative to *Tfap4*$^{+/+}$ cells. Reduction of *Erg* in *Tfap4*$^{+/+}$ cells did not have any additional effect on the expansion of transferred cells (Figure 6C,E). Also, reducing *Erg* expression rescued the differentiation of transferred *Tfap4*$^{+/-}$ MYC$^+$ pro/pre-B cells, as determined by the frequencies of IgM$^+$ cells (Figure 6F).

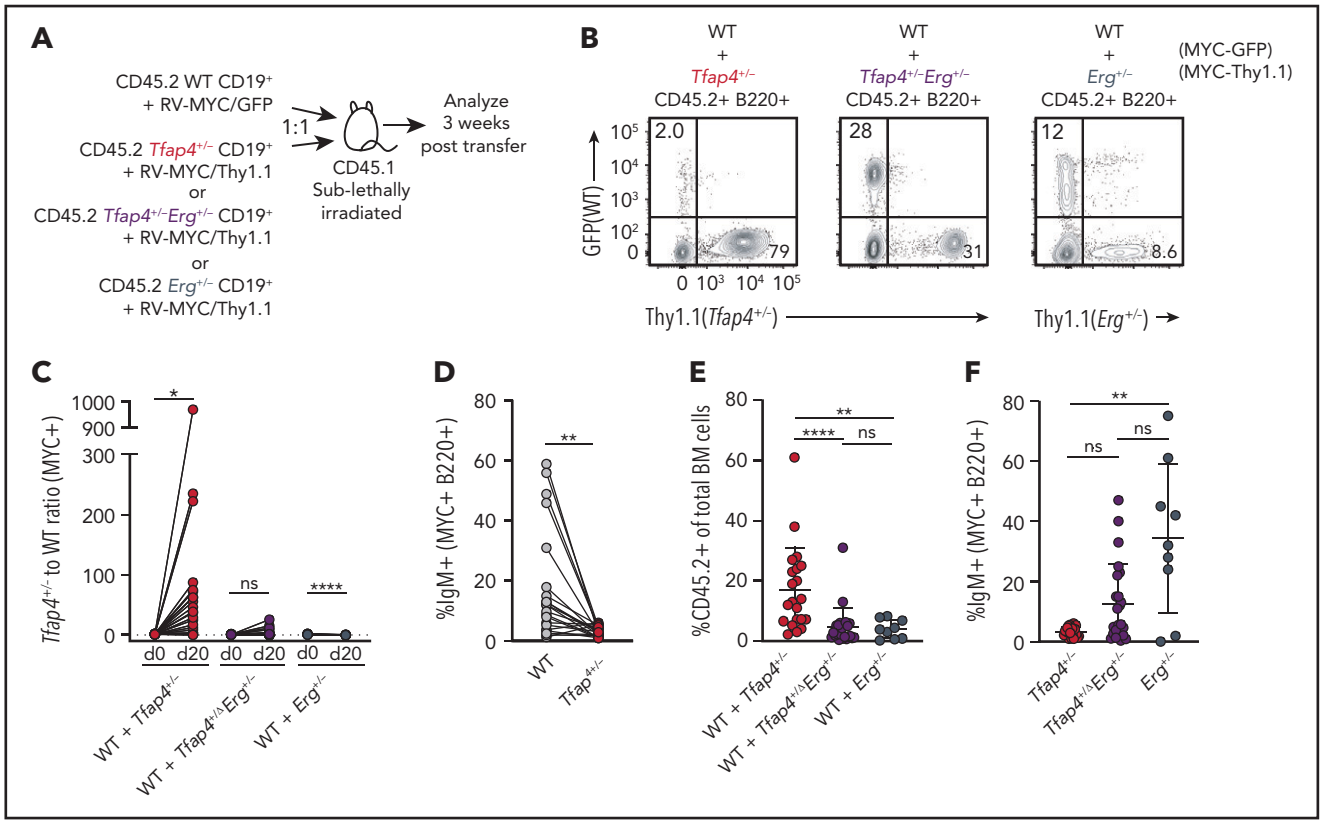

Figure 6. TFAP4-mediated restriction of *Erg* is required for coupling of c-MYC–dependent proliferation and differentiation. (A) Scheme for in vivo assessment of expansion and differentiation of *Tfap4*$^{+/+}$, *Tfap4*$^{+/-}$, *Tfap4*$^{+/-}$ *Erg*$^{+/-}$, and *Erg*$^{+/-}$ CD19^{+} pro/pre-B cells transduced with a distinct retrovirus encoding mouse c-MYC (T58A). MSCV-based retroviruses expressing mouse MYC-ires-GFP and mouse MYC-ires-Thy1.1 were packaged by transiently transfecting PlatE cells with a helper plasmid, pCL-10A1. Viral supernatant harvested 48 hours after transfection was used to infect freshly isolated CD45.2 CD19^{+} BM cells from 6- to 14-week-old mice (age matched within the experimental groups) with the indicated genotypes at 1000*g*, 30°C for 1.5 to 2 hours in the presence of 10 mg/mL Polybrene. Transduced CD19^{+} BM cells from *Tfap4*$^{+/+}$ (WT) and *Tfap4*$^{+/-}$ or *Tfap4*$^{+/-}$ *Erg*$^{+/-}$ or *Erg*$^{+/-}$ mice were cotransferred into sublethally irradiated CD45.1 recipients at a 1:1 ratio. Comparable infection efficiency across genotypes when using MYC-GFP or MYC-Thy1.1 retroviruses was achieved, as shown in supplemental Figure 6H. Three weeks later, mice were euthanized, and the proportions of each transduced cell population and their differentiation status were analyzed. (B) Representative flow cytometry plots showing frequencies of *Tfap4*$^{+/+}$ (WT) and *Tfap4*$^{+/-}$ (left panel), WT and *Tfap4*$^{+/-}$ *Erg*$^{+/-}$ (middle panel), and WT and *Erg*$^{+/-}$ (right panel) donor-derived B220^{+} cells in the BM of recipient mice 20 days after transfer. (C) Ratios of c-MYC–expressing *Tfap4*$^{+/-}$ to WT, *Tfap4*$^{+/-}$ *Erg*$^{+/-}$ to WT, and *Erg*$^{+/-}$ to WT cells in the BM of recipient mice 20 days after transfer. (D) Percentages of surface IgM^{+} transduced *Tfap4*$^{+/+}$ B220^{+} cells compared with *Tfap4*$^{+/-}$ B220^{+} cells in the same recipient mouse. (E) Percentages of CD45.2^{+} cells in the BM of mice in (A). (F) Percentages of surface IgM^{+} transduced *Tfap4*$^{+/-}$ B220^{+} cells compared with *Tfap4*$^{+/-}$ *Erg*$^{+/-}$ or *Erg*$^{+/-}$ B220^{+} cells (WT + *Tfap4*$^{+/-}$, n = 21; WT + *Tfap4*$^{+/-}$ *Erg*$^{+/-}$, n = 23; WT + *Erg*$^{+/-}$, n = 9), Data are from 3 independent experiments combined. *$P < .05$, **$P < .01$, ****$P < .0001$; paired Student *t* test (C-D), **$P < .01$, ****$P < .0001$; Kruskal -Wallis test with Dunn's multiple-comparison test (E,F). ns, no statistical significance.

TFAP4 is a positive prognosis factor in MYC-high B-ALL

So far, our data have demonstrated that TFAP4 is mutated in human B-cell malignancies, and reduced TFAP4 functionality predisposes proliferating B cells to transformation in preclinical models. To gain insights into the role of TFAP4 in c-MYC–driven B-cell malignancies in humans, we reanalyzed the expression of *c-MYC* and *TFAP4* in human pediatric B-ALL samples from the TARGET Phase II study (Figure 7A). Comparing patients with the top 25% and bottom 25% *TFAP4*/*MYC* ratios did not reveal a difference in the overall survival (data not shown). However, when we specifically compared samples with high *MYC* expression (z-score > 2), overall survival of patients with high *TFAP4* expression was better than that of patients with low *TFAP4* expression (Figure 7B-C). There was no difference in relative *ERG* expression between the 2 groups, possibly reflecting the selection of ERG-high clones during disease progression. Alternatively, the result also suggests an additional ERG-independent control of ALL progression by TFAP4 or ERG regulation by other oncogenic pathways (Figure 7D). These results suggest that upregulation of TFAP4 by c-MYC is a decisive factor for predisposition to B-cell malignancies, as well as is associated with the prognosis for patients with B-ALL.

Discussion

Our study provides compelling evidence that c-MYC engages a tumor-suppressive program in B cells by inducing its direct downstream factor TFAP4. Coding mutations of *TFAP4* prevail in lymphoid malignancies, particularly in a significant proportion of cases of BL. Our mouse models reveal substantial impacts on tumor onset by deletion or reduced expression of *Tfap4* in developing B cells and mature B cells in the face of aberrant *Myc* expression. The tumor suppression is mediated, at least in part, by restricting the stemness factor ERG in immature B cells, because

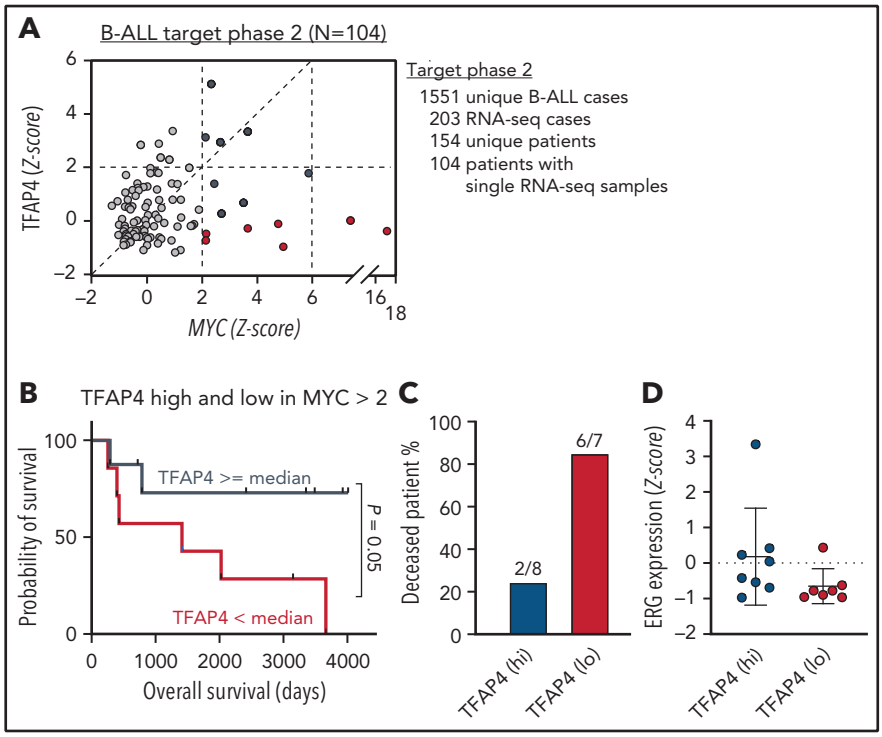

Figure 7. TFAP4 is a positive prognosis factor in B-ALL. (A) Plot showing normalized *MYC* and *TFAP4* expression from 104 B-ALL patient samples in the TARGET phase 2 study. (B-C) Survival analysis of deceased patients with high vs low *TFAP4* expression among patients with high *MYC* expression (z score >2; $TFAP4^{lo}$ median survival, 1413 days; $TFAP4^{hi}$ median survival, undefined). (D) Normalized *ERG* expression from B-ALL patient samples in (B). RNA-seq, RNA sequencing.

the reduced expression of *Erg* was sufficient to rescue developing B cells from aberrant expansion and accelerated transformation.

During hematopoiesis, HSCs give rise to various mature subsets through defined pathways. Because several proto-oncogenes are essential for normal hematopoiesis, their expression levels and timing must be tightly regulated to restrict the risk of leukemogenesis. Nonetheless, clonal hematopoiesis carrying oncogenic translocations is found in healthy individuals at a higher incidence than that of corresponding leukemias, including the t(8;14) translocation modeled by Eμ-*Myc* mice.[54–56] Therefore, appropriate engagement of tumor suppression is essential to prevent these clones from transformation. HSCs and undifferentiated progenitors generate greater numbers of mature progenies through proliferation that is tightly linked to differentiation and at the cost of their self-renewing potential. Thus, perturbation of normal differentiation could result in a decoupling of the loss of self-renewal capacity and proliferation, which has been associated with hematopoietic malignancies.[57–63] In HSCs, the antagonistic interplay between c-MYC and ERG is essential for balancing self-renewal and differentiation.[41] ERG is essential for self-renewal of undifferentiated HSCs through suppression of c-MYC target genes; accordingly, loss of ERG closely recapitulates c-MYC overexpression in HSCs, resulting in depletion of undifferentiated HSCs.[41,53] We demonstrate that the balance between MYC and ERG controls self-renewal and differentiation of B-cell progenitors. Insufficient TFAP4 induction and subsequent *Erg* persistence selectively impair the differentiation program by c-MYC, allowing c-MYC–expressing cells to continue proliferation with an undifferentiated phenotype and eventually form tumors. Although a subset of B-ALL is characterized by reduced ERG activity that is likely caused by an independent mechanism, elevated *ERG* was noted in a majority of cases of B-ALL that also express elevated c-MYC.

The frequency of *TFAP4* mutations is rare in human B-ALL. However, within *MYC*-high B-ALL cases, the level of *TFAP4* expression is associated with patient prognosis. Because increased *TFAP4* expression is associated with poor prognosis in some cancers,[64–66] lymphocytes may have established unique gene expression circuitry that converts the c-MYC–TFAP4 axis from a proproliferative/tumorigenesis module into a tumor-suppressive module by restricting their distinct targets. Similar counterregulation of MYC-driven proliferation may also be involved in the suppression of lymphomagenesis in GCB cells. GCB cells retain high proliferative potential similar to pro/pre-B cells, and TFAP4 may analogously function as a tumor suppressor by tightly coupling the expression of MYC and the restriction of continued proliferation. Thus, the induction of TFAP4 by MYC impacts the predisposition of B-cell malignancies, as well as likely contributes to disease progression. A therapeutic benefit for B-cell malignancies marked by high *MYC* expression and low *TFAP4* could be achieved by inhibiting SCF ubiquitin ligase, leading to general cell cycle inhibition and specific stabilization of TFAP4, thus increasing the level of TFAP4 and balancing MYC and TFAP4 levels.[67,68] We uncover that perturbation of the c-MYC–initiated and TFAP4-mediated feedback mechanism dramatically accelerates tumorigenesis.

Acknowledgments

The authors thank Vivek Durai, Sunnie Hsiung, Tenzin Yangdon, Jason Walker, and Mike White for technical support; Barry Sleckman for MYC-GFP mice; Kenneth Murphy, Eugene Oltz, Jacqueline Payton, and Dan

Littman for discussions and critical reading of the manuscript; the Maxim Artyomov laboratory for the development of the RNA sequencing analysis tool Phantasus; and the Genome Technology Access Center (Department of Genetics, Washington University School of Medicine) for help with genomic analyses.

This work was supported by National Institutes of Health (NIH), National Institute of Allergy and Infectious Diseases grants R56 AI114593-01A1 (T.E.) and R01 AI130152-01A1 (T.E.), and NIH, National Institute of Arthritis and Musculoskeletal and Skin Diseases (NIAMS) grant R01 AR046000 (M.I.); Leukemia and Lymphoma Society Scholar Award 1349-18 (T.E.); a Siteman Investment Program Research Development Award (T.E.); and a Hu and Zeng Predoctoral Scholarship (E.T.). The Washington University Rheumatic Diseases Research Resource-based Center is supported by NIH, NIAMS grant P30 AR073752. The Genome Technology Access Center is supported, in part, by NIH, National Cancer Institute Cancer Center Support Grant P30CA91842 to the Siteman Cancer Center, and by the Institute of Clinical and Translational Sciences/Clinical and Translational Science Award (UL1TR000448) from the National Center for Research Resources, a component of the NIH, and the NIH Roadmap for Medical Research.

Authorship

Contribution: T.E. conceived the project; E.T., C.C., and T.E. designed experiments and interpreted the results; E.T., Y.T., C.C., Y.X., M.H., C.F., S.R., and T.E. performed experiments; G.S.C. helped with the analysis of whole-exome sequencing data; M.I. provided *Erg*-flox mice; and E.T. and T.E. wrote the manuscript with editorial comments from all of the other authors.

Conflict-of-interest disclosure: T.E. and C.C. have filed a provisional US patent application to propose the use of stabilized TFAP4 to improve T-cell function (Application Number 16343951 "AP4 and Methods of Promoting T Cell Activation"). The remaining authors declare no competing financial interests.

ORCID profiles: E.T., 0000-0002-6604-6496; T.E., 0000-0001-7489-1051.

Correspondence: Takeshi Egawa, Washington University in St Louis, 660 South Euclid Ave, Campus Box 8118, St. Louis, MO 63110; e-mail: egawat@wustl.edu.

Footnotes

Submitted 15 March 2021; accepted 10 July 2021; prepublished online on *Blood* First Edition 20 July 2021. DOI 10.1182/blood.2021011711.

The sequencing data reported in this article have been deposited in the National Center for Biotechnology Information Gene Expression Omnibus and Sequence Read Archive (accession numbers GSE133514 and PRJNA551263).

Data sharing requests should be sent to Takeshi Egawa (egawat@wustl.eu).

The online version of this article contains a data supplement.

The publication costs of this article were defrayed in part by page charge payment. Therefore, and solely to indicate this fact, this article is hereby marked "advertisement" in accordance with 18 USC section 1734.

REFERENCES

1. Gitlin AD, Mayer CT, Oliveira TY, et al. HUMORAL IMMUNITY. T cell help controls the speed of the cell cycle in germinal center B cells. *Science*. 2015;349(6248):643-646.
2. Victora GD, Nussenzweig MC. Germinal centers. *Annu Rev Immunol*. 2012;30(1):429-457.
3. Goldrath AW, Bevan MJ. Selecting and maintaining a diverse T-cell repertoire. *Nature*. 1999;402(6759):255-262.
4. Melchers F. Checkpoints that control B cell development. *J Clin Invest*. 2015;125(6):2203-2210.
5. Mesin L, Ersching J, Victora GD. Germinal center B cell dynamics. *Immunity*. 2016;45(3):471-482.
6. De Silva NS, Klein U. Dynamics of B cells in germinal centres. *Nat Rev Immunol*. 2015;15(3):137-148.
7. Mahowald GK, Baron JM, Sleckman BP. Collateral damage from antigen receptor gene diversification. *Cell*. 2008;135(6):1009-1012.
8. National Cancer Institute. Surveillance, Epidemiology, and End Results Program. Cancer Stat Facts. Available at: https://seer.cancer.gov/statfacts. Accessed 19 June 2019.
9. Carroll PA, Freie BW, Mathsyaraja H, Eisenman RN. The MYC transcription factor network: balancing metabolism, proliferation and oncogenesis. *Front Med*. 2018;12(4):412-425.
10. Gabay M, Li Y, Felsher DW. MYC activation is a hallmark of cancer initiation and maintenance. *Cold Spring Harb Perspect Med*. 2014;4(6):a014241.
11. Stine ZE, Walton ZE, Altman BJ, Hsieh AL, Dang CV. MYC, metabolism, and cancer. *Cancer Discov*. 2015;5(10):1024-1039.
12. Calado DP, Sasaki Y, Godinho SA, et al. The cell-cycle regulator c-Myc is essential for the formation and maintenance of germinal centers. *Nat Immunol*. 2012;13(11):1092-1100.
13. Dominguez-Sola D, Victora GD, Ying CY, et al. The proto-oncogene MYC is required for selection in the germinal center and cyclic reentry. *Nat Immunol*. 2012;13(11):1083-1091.
14. Wang R, Dillon CP, Shi LZ, et al. The transcription factor Myc controls metabolic reprogramming upon T lymphocyte activation. *Immunity*. 2011;35(6):871-882.
15. de Alboran IM, O'Hagan RC, Gärtner F, et al. Analysis of C-MYC function in normal cells via conditional gene-targeted mutation. *Immunity*. 2001;14(1):45-55.
16. Chou C, Pinto AK, Curtis JD, et al. c-Myc-induced transcription factor AP4 is required for host protection mediated by CD8+ T cells. *Nat Immunol*. 2014;15(9):884-893.
17. Chou C, Verbaro DJ, Tonc E, et al. The transcription factor AP4 mediates resolution of chronic viral infection through amplification of germinal center B cell responses. *Immunity*. 2016;45(3):570-582.
18. Egawa T, Littman DR. Transcription factor AP4 modulates reversible and epigenetic silencing of the Cd4 gene. *Proc Natl Acad Sci USA*. 2011;108(36):14873-14878.
19. Ohta Y, Okabe T, Larmour C, et al. Articular cartilage endurance and resistance to osteoarthritic changes require transcription factor Erg. *Arthritis Rheumatol*. 2015;67(10):2679-2690.
20. Hobeika E, Thiemann S, Storch B, et al. Testing gene function early in the B cell lineage in mb1-cre mice. *Proc Natl Acad Sci USA*. 2006;103(37):13789-13794.
21. Huang CYB, Bredemeyer AL, Walker LM, Bassing CH, Sleckman BP. Dynamic regulation of c-Myc proto-oncogene expression during lymphocyte development revealed by a GFP-c-Myc knock-in mouse. *Eur J Immunol*. 2008;38(2):342-349.
22. Adams JM, Harris AW, Pinkert CA, et al. The c-myc oncogene driven by immunoglobulin enhancers induces lymphoid malignancy in transgenic mice. *Nature*. 1985;318(6046):533-538.
23. Casola S, Cattoretti G, Uyttersprot N, et al. Tracking germinal center B cells expressing germ-line immunoglobulin γ1 transcripts by conditional gene targeting [published correction appears in *Proc Natl Acad Sci USA*. 2007;104(6):2025]. *Proc Natl Acad Sci USA*. 2006;103(19):7396-7401.
24. Sander S, Calado DP, Srinivasan L, et al. Synergy between PI3K signaling and MYC in Burkitt lymphomagenesis. *Cancer Cell*. 2012;22(2):167-179.
25. Srinivasan L, Sasaki Y, Calado DP, et al. PI3 kinase signals BCR-dependent mature B cell survival. *Cell*. 2009;139(3):573-586.
26. Panea RI, Love CL, Shingleton JR, et al. The whole-genome landscape of Burkitt lymphoma subtypes. *Blood*. 2019;134(19):1598-1607.

27. Zenkova D, Kamenev V, Sablina R, Artyomov M, Sergushichev A. Phantasus: visual and interactive gene expression analysis. https://genome.ifmo.ru/phantasus

28. Sabò A, Kress TR, Pelizzola M, et al. Selective transcriptional regulation by Myc in cellular growth control and lymphomagenesis. *Nature*. 2014;511(7510):488-492.

29. Hu YF, Lüscher B, Admon A, Mermod N, Tjian R. Transcription factor AP-4 contains multiple dimerization domains that regulate dimer specificity. *Genes Dev*. 1990;4(10):1741-1752.

30. Jung P, Menssen A, Mayr D, Hermeking H. AP4 encodes a c-MYC-inducible repressor of p21. *Proc Natl Acad Sci USA*. 2008;105(39):15046-15051.

31. Egle A, Harris AW, Bouillet P, Cory S. Bim is a suppressor of Myc-induced mouse B cell leukemia. *Proc Natl Acad Sci USA*. 2004;101(16):6164-6169.

32. Kotani A, Kakazu N, Tsuruyama T, et al. Activation-induced cytidine deaminase (AID) promotes B cell lymphomagenesis in Emu-cmyc transgenic mice. *Proc Natl Acad Sci USA*. 2007;104(5):1616-1620.

33. Liu Y, Chen C, Xu Z, et al. Deletions linked to TP53 loss drive cancer through p53-independent mechanisms. *Nature*. 2016;531(7595):471-475.

34. Hemann MT, Bric A, Teruya-Feldstein J, et al. Evasion of the p53 tumour surveillance network by tumour-derived MYC mutants. *Nature*. 2005;436(7052):807-811.

35. Subramanian A, Tamayo P, Mootha VK, et al. Gene set enrichment analysis: a knowledge-based approach for interpreting genome-wide expression profiles. *Proc Natl Acad Sci USA*. 2005;102(43):15545-15550.

36. Liberzon A, Subramanian A, Pinchback R, et al. Molecular signatures database (MSigDB) 3.0. *Bioinformatics*. 2011;27(12):1739-1740.

37. Liberzon A, Birger C, Thorvaldsdóttir H, et al. The Molecular Signatures Database (MSigDB) hallmark gene set collection. *Cell Syst*. 2015;1(6):417-425.

38. Kortlever RM, Sodir NM, Wilson CH, et al. Myc cooperates with Ras by programming inflammation and immune suppression. *Cell*. 2017;171(6):1301-1315.e14.

39. Lefebure M, Tothill RW, Kruse E, et al. Genomic characterisation of Eμ-Myc mouse lymphomas identifies Bcor as a Myc co-operative tumour-suppressor gene. *Nat Commun*. 2017;8(1):14581.

40. Morton JP, Sansom OJ. MYC-y mice: from tumour initiation to therapeutic targeting of endogenous MYC. *Mol Oncol*. 2013;7(2):248-258.

41. Knudsen KJ, Rehn M, Hasemann MS, et al. ERG promotes the maintenance of hematopoietic stem cells by restricting their differentiation. *Genes Dev*. 2015;29(18):1915-1929.

42. Bock J, Mochmann LH, Schlee C, et al. ERG transcriptional networks in primary acute leukemia cells implicate a role for ERG in deregulated kinase signaling. *PLoS One*. 2013;8(1):e52872.

43. Thoms JA, Birger Y, Foster S, et al. ERG promotes T-acute lymphoblastic leukemia and is transcriptionally regulated in leukemic cells by a stem cell enhancer. *Blood*. 2011;117(26):7079-7089.

44. Tsuzuki S, Taguchi O, Seto M. Promotion and maintenance of leukemia by ERG. *Blood*. 2011;117(14):3858-3868.

45. Zhang J, McCastlain K, Yoshihara H, et al; St. Jude Children's Research Hospital–Washington University Pediatric Cancer Genome Project. Deregulation of DUX4 and ERG in acute lymphoblastic leukemia. *Nat Genet*. 2016;48(12):1481-1489.

46. Zhao HZ, Jia M, Luo ZB, et al. ETS-related gene is a novel prognostic factor in childhood acute lymphoblastic leukemia. *Oncol Lett*. 2017;13(1):455-462.

47. Andersson A, Ritz C, Lindgren D, et al. Microarray-based classification of a consecutive series of 121 childhood acute leukemias: prediction of leukemic and genetic subtype as well as of minimal residual disease status. *Leukemia*. 2007;21(6):1198-1203.

48. Armstrong SA, Staunton JE, Silverman LB, et al. MLL translocations specify a distinct gene expression profile that distinguishes a unique leukemia. *Nat Genet*. 2002;30(1):41-47.

49. Ramaswamy S, Tamayo P, Rifkin R, et al. Multiclass cancer diagnosis using tumor gene expression signatures. *Proc Natl Acad Sci USA*. 2001;98(26):15149-15154.

50. Maia S, Haining WN, Ansén S, et al. Gene expression profiling identifies BAX-delta as a novel tumor antigen in acute lymphoblastic leukemia. *Cancer Res*. 2005;65(21):10050-10058.

51. Ma X, Liu Y, Liu Y, et al. Pan-cancer genome and transcriptome analyses of 1,699 paediatric leukaemias and solid tumours. *Nature*. 2018;555(7696):371-376.

52. Søndergaard E, Rauch A, Michaut M, et al. ERG controls B cell development by promoting Igh V-to-DJ recombination. *Cell Rep*. 2019;29(9):2756-2769.e6.

53. Wilson A, Murphy MJ, Oskarsson T, et al. c-Myc controls the balance between hematopoietic stem cell self-renewal and differentiation. *Genes Dev*. 2004;18(22):2747-2763.

54. Schäfer D, Olsen M, Lähnemann D, et al. Five percent of healthy newborns have an *ETV6-RUNX1* fusion as revealed by DNA-based GIPFEL screening. *Blood*. 2018;131(7):821-826.

55. Ismail SI, Naffa RG, Yousef AM, Ghanim MT. Incidence of bcr-abl fusion transcripts in healthy individuals. *Mol Med Rep*. 2014;9(4):1271-1276.

56. Janz S, Potter M, Rabkin CS. Lymphoma- and leukemia-associated chromosomal translocations in healthy individuals. *Genes Chromosomes Cancer*. 2003;36(3):211-223.

57. Seita J, Weissman IL. Hematopoietic stem cell: self-renewal versus differentiation. *Wiley Interdiscip Rev Syst Biol Med*. 2010;2(6):640-653.

58. Jamieson CH, Ailles LE, Dylla SJ, et al. Granulocyte-macrophage progenitors as candidate leukemic stem cells in blast-crisis CML. *N Engl J Med*. 2004;351(7):657-667.

59. Cornic M, Agadir A, Degos L, Chomienne C. Retinoids and differentiation treatment: a strategy for treatment in cancer. *Anticancer Res*. 1994;14(6A):2339-2346.

60. Dos Santos GA, Kats L, Pandolfi PP. Synergy against PML-RARa: targeting transcription, proteolysis, differentiation, and self-renewal in acute promyelocytic leukemia. *J Exp Med*. 2013;210(13):2793-2802.

61. Ablain J, de The H. Revisiting the differentiation paradigm in acute promyelocytic leukemia. *Blood*. 2011;117(22):5795-5802.

62. Welch JS, Yuan W, Ley TJ. PML-RARA can increase hematopoietic self-renewal without causing a myeloproliferative disease in mice. *J Clin Invest*. 2011;121(4):1636-1645.

63. de Thé H, Chen Z. Acute promyelocytic leukaemia: novel insights into the mechanisms of cure. *Nat Rev Cancer*. 2010;10(11):775-783.

64. Boboila S, Lopez G, Yu J, et al. Transcription factor activating protein 4 is synthetically lethal and a master regulator of MYCN-amplified neuroblastoma. *Oncogene*. 2018;37(40):5451-5465.

65. Jackstadt R, Röh S, Neumann J, et al. AP4 is a mediator of epithelial-mesenchymal transition and metastasis in colorectal cancer. *J Exp Med*. 2013;210(7):1331-1350.

66. Jaeckel S, Kaller M, Jackstadt R, et al. Ap4 is rate limiting for intestinal tumor formation by controlling the homeostasis of intestinal stem cells. *Nat Commun*. 2018;9(1):3573.

67. Gorelik M, Orlicky S, Sartori MA, et al. Inhibition of SCF ubiquitin ligases by engineered ubiquitin variants that target the Cul1 binding site on the Skp1-F-box interface. *Proc Natl Acad Sci USA*. 2016;113(13):3527-3532.

68. D'Annibale S, Kim J, Magliozzi R, et al. Proteasome-dependent degradation of transcription factor activating enhancer-binding protein 4 (TFAP4) controls mitotic division. *J Biol Chem*. 2014;289(11):7730-7737.